

Comparative Hypothesis Testing of Auroral L-Band Scintillation Layer

Gytis Blinstrubas¹ (gblinstrubas@hawk.iit.edu), Alex English¹,

David Stuart¹, Don Hampton², Leslie Lamarche³, Yukitoshi Nishimura⁴, Seebany Datta-Barua¹

¹Illinois Institute of Technology, Chicago, IL, USA, ²University of Alaska Fairbanks, Fairbanks, AK, USA,

³SRI International, Menlo Park, CA, USA, ⁴Boston University, Boston, MA, USA



ILLINOIS INSTITUTE OF TECHNOLOGY



Introduction

Motivation: Scattering layers of GNSS (Global Navigation Satellite System) are normally hypothesized using case studies

Objective: Determine the layer where scintillation will likely occur using a survey of scintillation events

Background

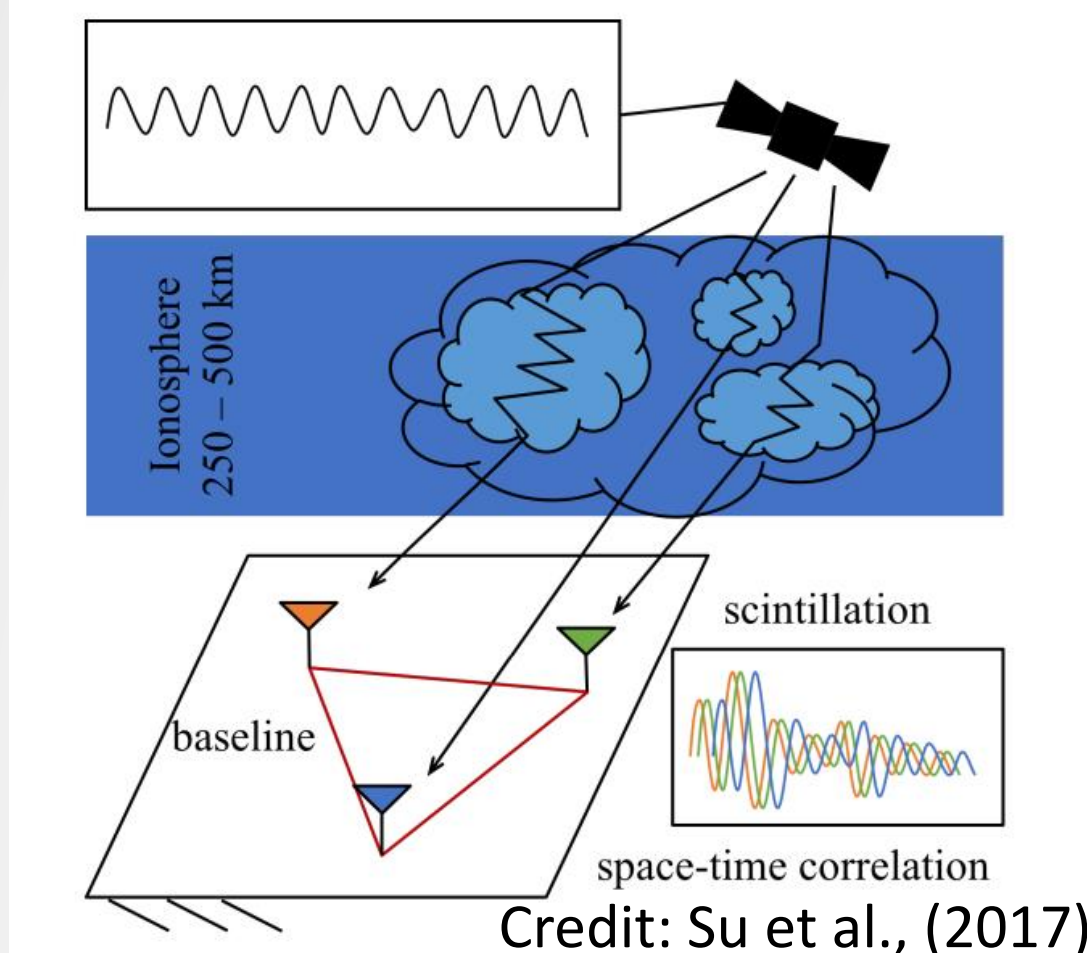


Fig 1.) Image describing scintillation

- Scintillation Auroral GPS Array (SAGA) is used to detect when scintillation occurs (Sreenivash et al., 2020)
- ~ 5,000 scintillation events analyzed in this study
- Sreenivash et al. 2020 hypothesize where peak electron densities occur is where the scattering layer is likeliest to be

- Ratios of auroral light emission can also be used to predict the scattering layer
- Multi-instrument study used to hypothesis layers

Instrumentation

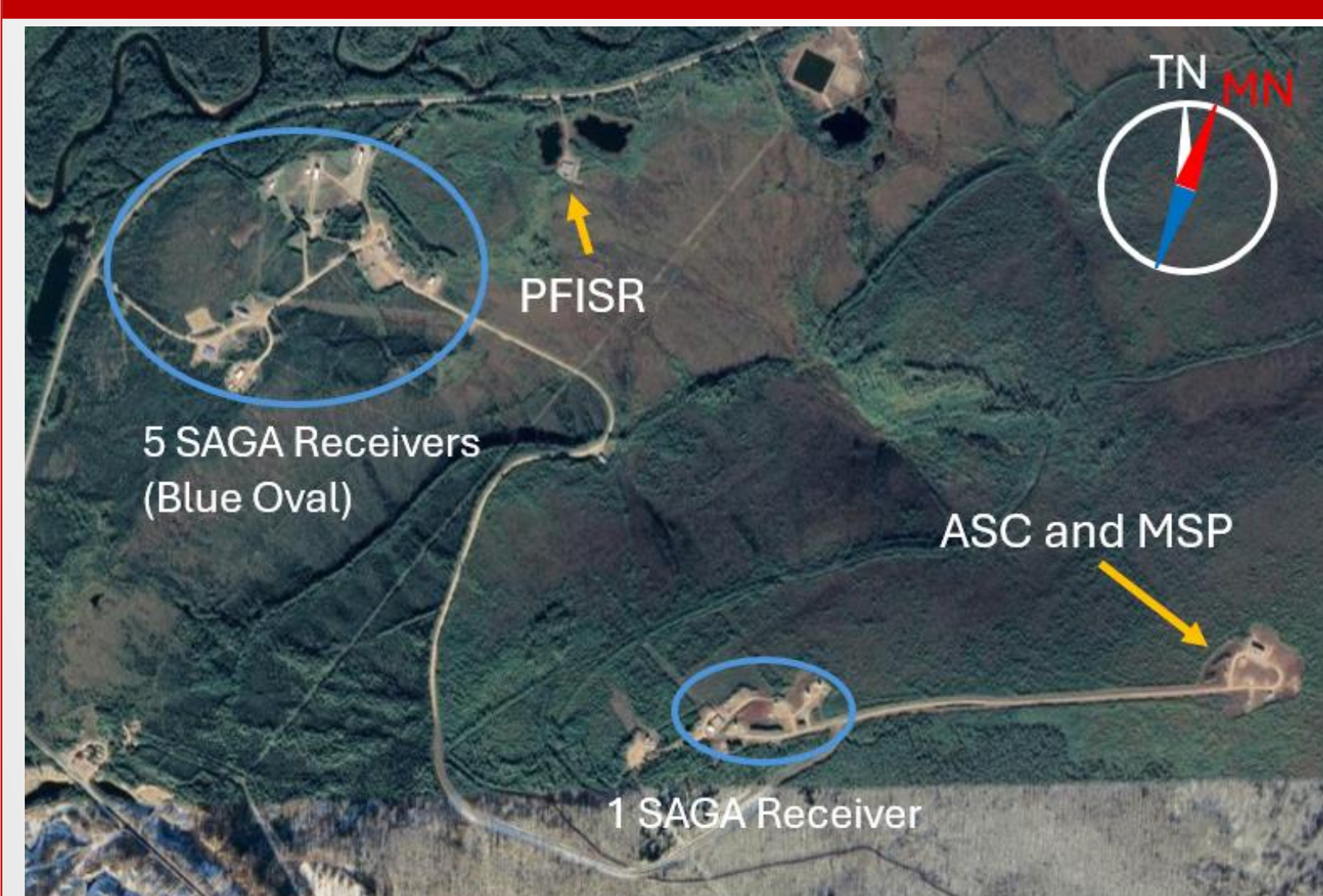


Fig 2.) Location of instruments at Poker Flat Image Modified from Google Earth

PFISR

- Instruments located at Poker Flat Research Range
- (66.1°N magnetic)
- Poker Flat Incoherent Scatter Radar (PFISR) measures electron densities
- All-sky Cameras (ASC) measure emission related to particle precipitation
- Southward facing, anti-parallel to local magnetic field line (205.7° az, 77.5° el) beam used
- Two types of electron density data used
 - Long Pulse (LP) (above 195 km)
 - Alternating Code (AC) (below 195 km)

ASC

- 2-D image from white light camera
- Two physical filters
 - 428 nm (blue) filter (excitation of N_2^+ - E Region)⁷
 - 630 nm (red) filter ($O(1D)$ - F Region)⁷

$$M_{\lambda,ij}(t) = (S_{\lambda,ij}(t) - \beta_{\lambda}) \left(\frac{k_{\lambda}}{\tau_{\lambda}} \right)$$

- The corrected photon flux M (Rayleighs) at wavelength λ , (i,j) are the pixel indices
- S is the raw sensor image (camera counts)
- β_{λ} is a constant bias (camera counts)
- k_{λ} is a camera response per exposure time
- τ is the camera exposure time



Fig 3.) Image using an all-sky imager

Method

Density-based hypothesis:

PFISR electron density data used to find peak electron densities

Step 1.) Check if at least 80% of AC data and 80% of LP data is available during scintillation

Step 2.) Filter out data points if $DNe > \frac{Ne}{3}$ (LP data), $DNe > Ne$ (AC data)

(gray oval Fig. 5)

Step 3.) Find maximum electron densities for each time step PFISR outputs data (red oval Fig 5)

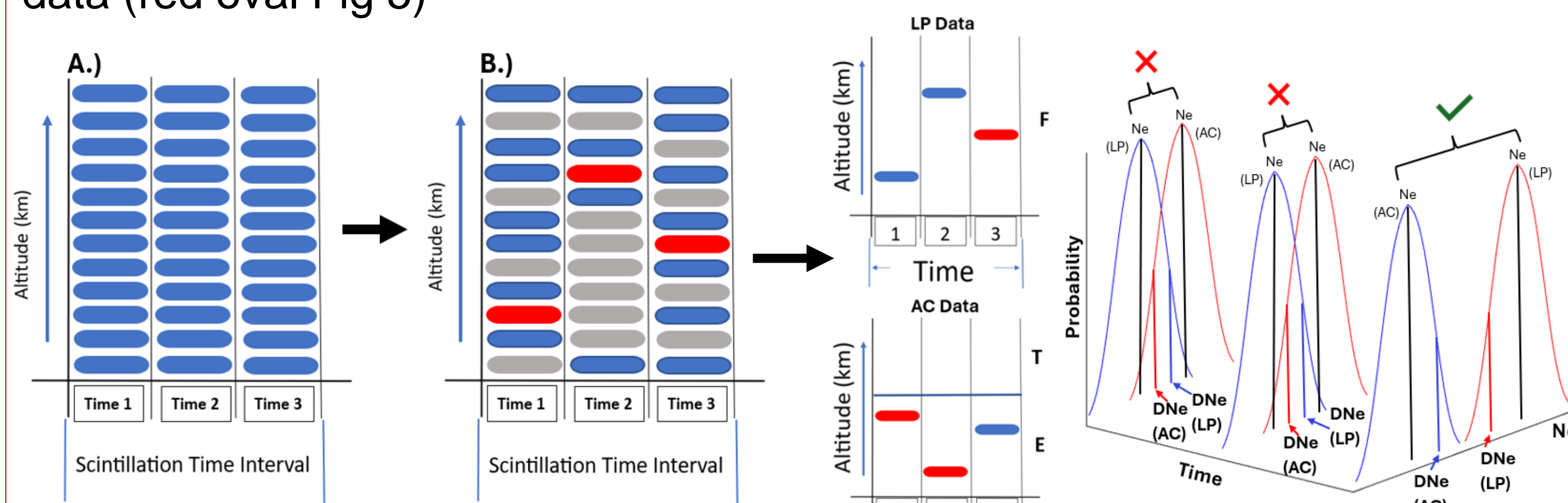


Fig 4.) Cartoon of data filtering due to uncertainty criteria. Red ovals (max densities), gray ovals (data filtered out due to large uncertainties)

Fig 5.) Process showing when measurement uncertainties overlap

Step 4.) At time t let Ne_1 be the greater density measurement ($Ne_1 > Ne_2$) if $Ne_1 - DNe_1 < Ne_2 + DNe_2$ the measurements fall within each others uncertainty and all data is removed at that time step

Step 5.) Compare remaining peak densities from AC data to LP data

Energy-based Hypothesis:

ASC is used to measure emissions of aurora

Step 1.)

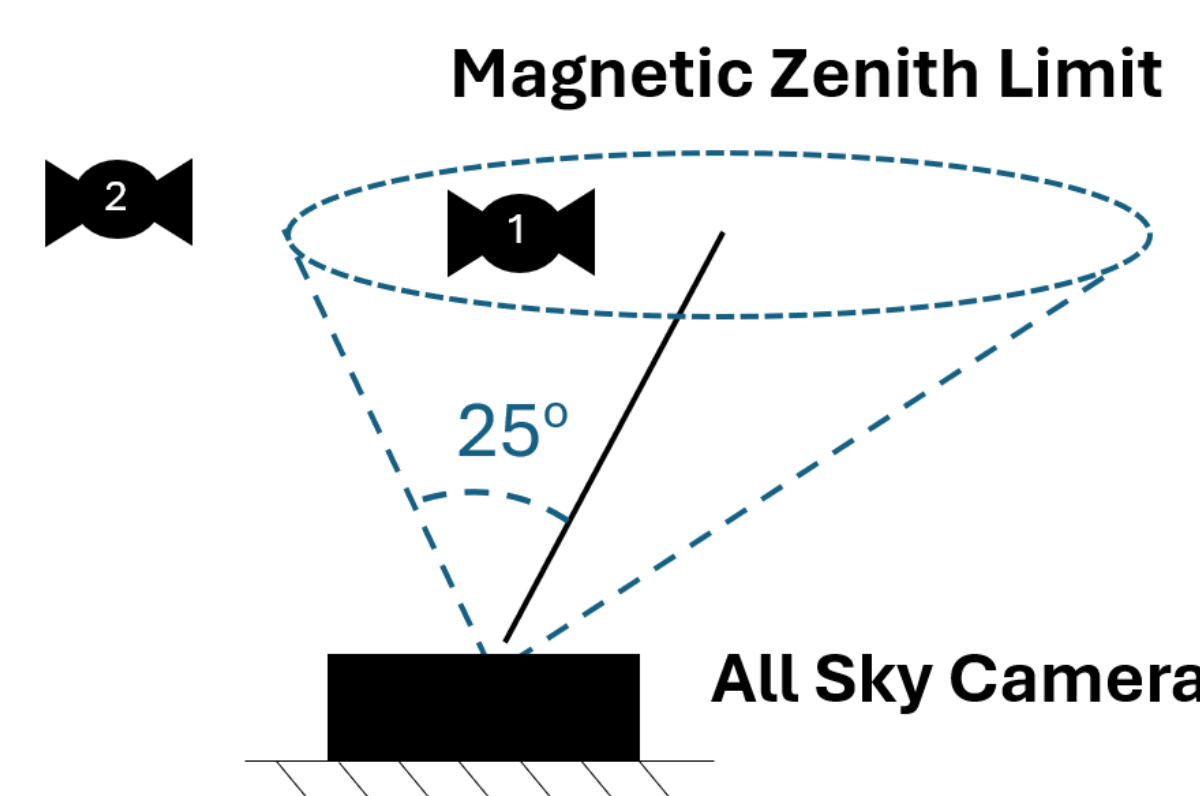


Fig 6.) Remove satellites not within magnetic zenith limit

Step 2.)

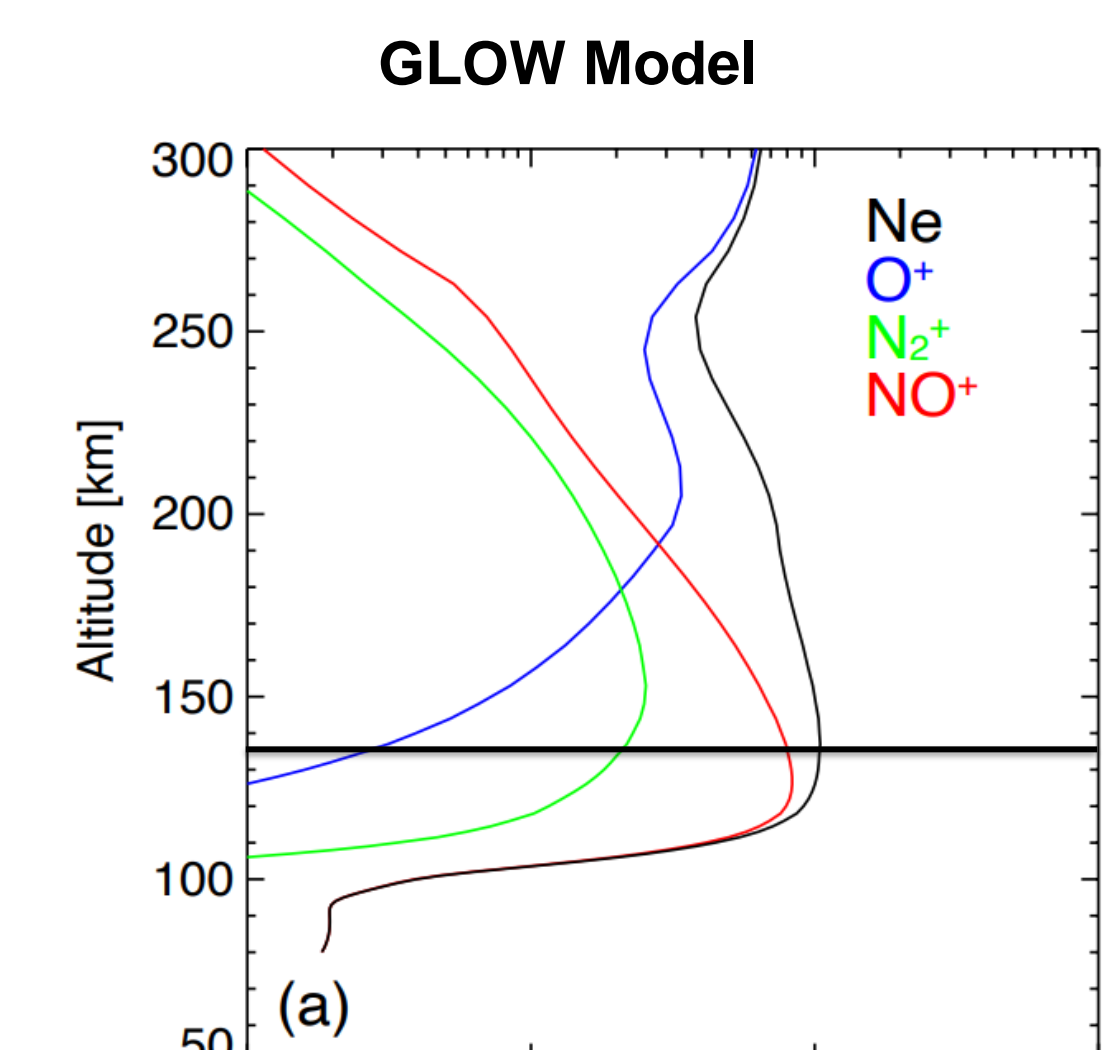


Fig 7.) GLOW model Output: Image Credit: Dr. Nishimura

Step 3.)

$$\rho_{630/428}(t) = \frac{M_{630.0}}{M_{428.0}}$$

- Use the ratio of the ASI red image (630.0 nm) pixel intensity to the blue (428.0 nm) pixel intensity
- Red/Blue ratio of 1.35 corresponds to E/F region cutoff of 135 km

Step 4.)

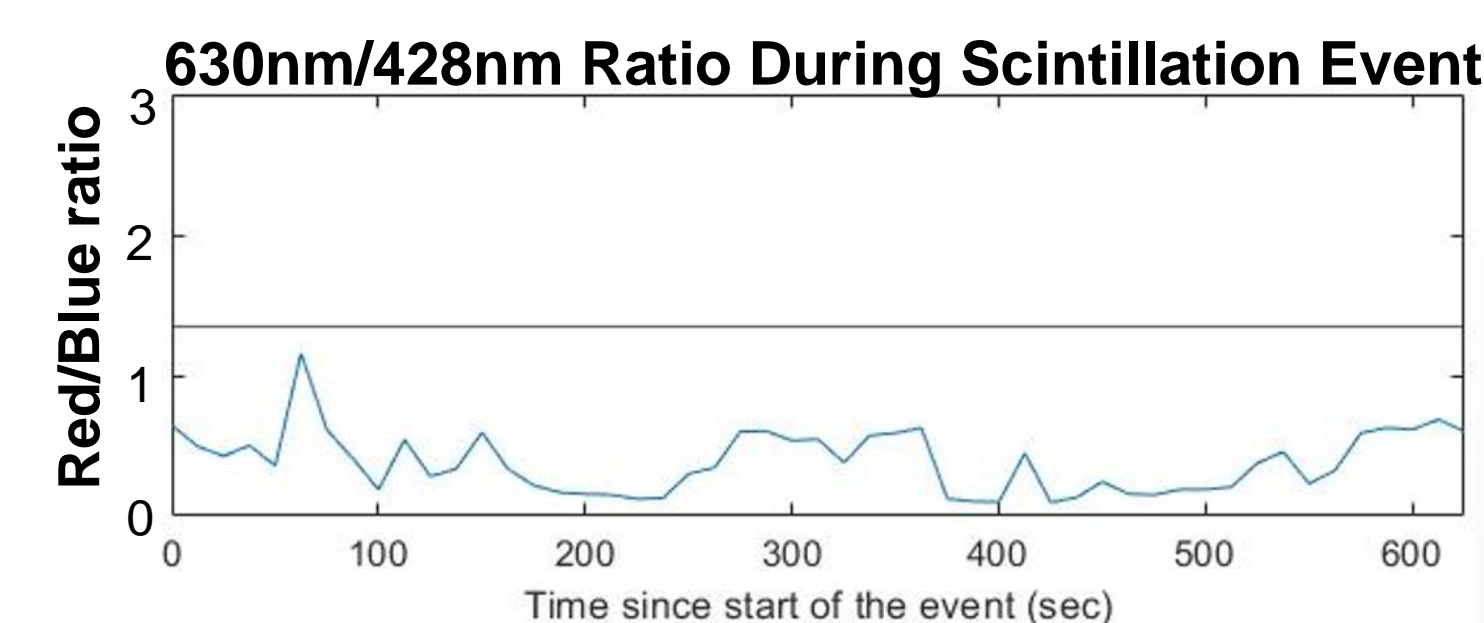


Fig 8.) 630nm/428nm ratio during scintillation event occurring on 03/18/2015.

Results

Density Method Layer

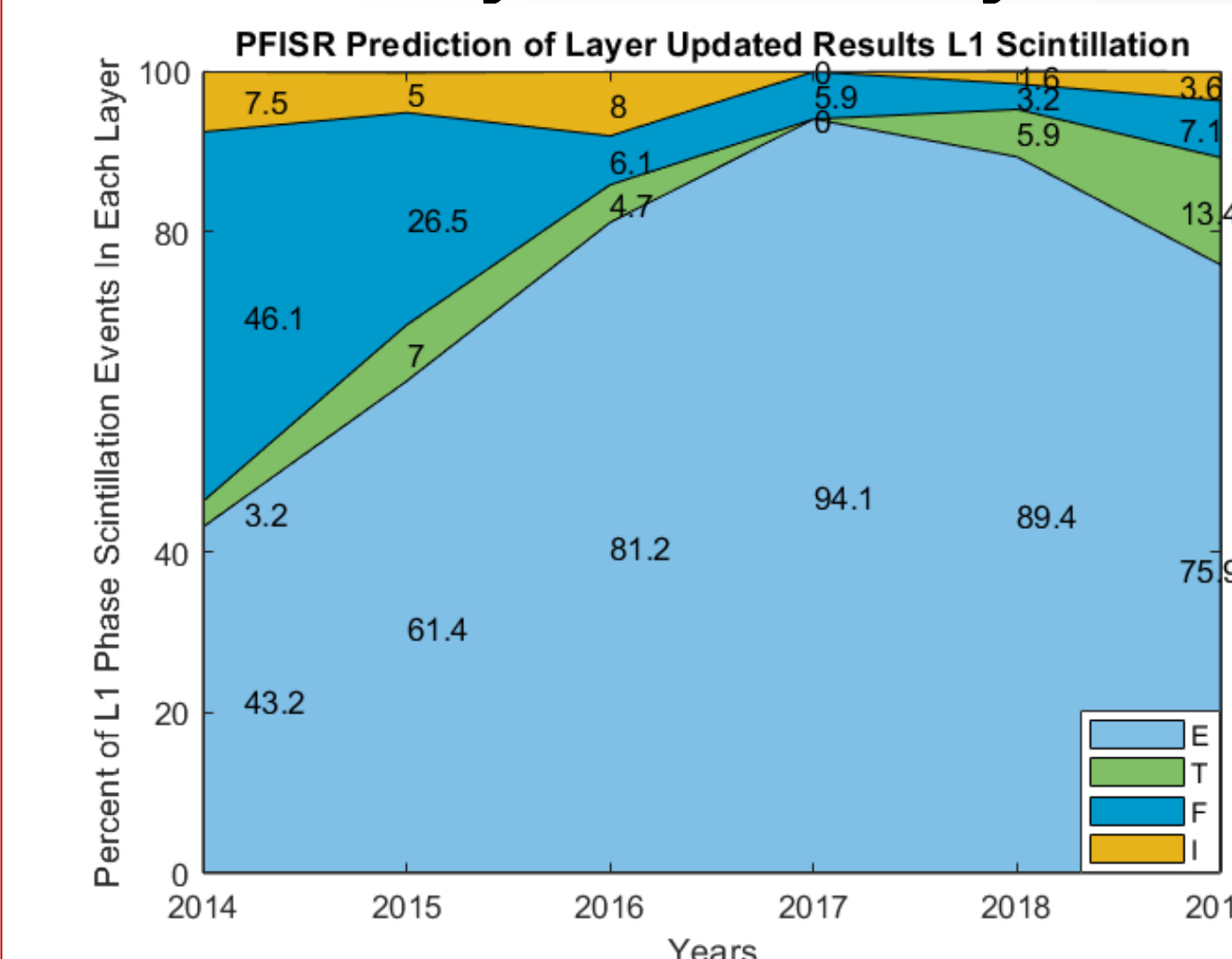


Fig 9.) Results of density-based method as a percentage year-by-year

Energy Method Layer

| L1 | | | |
|-------|----|----|-------|
| Year | E | F | Total |
| 2014 | 53 | 15 | 68 |
| 2015 | 13 | 6 | 19 |
| 2016 | 11 | 2 | 13 |
| 2017 | 5 | 0 | 5 |
| 2018 | 6 | 0 | 6 |
| Total | 88 | 23 | 111 |

| L2C | | | |
|-------|----|----|-------|
| Year | E | F | Total |
| 2014 | 28 | 6 | 34 |
| 2015 | 9 | 5 | 14 |
| 2016 | 8 | 0 | 8 |
| 2017 | 5 | 0 | 5 |
| 2018 | 2 | 0 | 2 |
| Total | 52 | 11 | 63 |

Table 1.) Results of energy-based method: most layers are categorized as E events

Comparison of Density to Energy Based Method

| Total Events = 174 | | Density Based | |
|--------------------|---|---------------|----------|
| | | E | F |
| Energy Based | E | 114 (65%) | 26 (15%) |
| | F | 19 (11%) | 15 (9%) |

Table 2.) Comparison of density-based method to energy-based method

- Survey 174 events from 2014-2018
- PFISR ASI Agree 74% and disagree 26%
- Majority of scintillation occurs in E region

Conclusion

- Updated the density-base method to more accurately predict irregularity layers
- Used the all-sky imager to predict irregularity layers due to precipitating electrons
- **Scintillation likeliest to occur in E region**
- **Future Work:**
 - Case study analysis of events when the density-based and energy-based methods disagree

Acknowledgments

NSF AGS-1651465 and NASA award 80NSSC21K1354 supported this work. CEDAR Student Travel Support, ISR Workshop travel support. Vaishnavi Sreenivash, Yang Su, Pablo Reyes PFISR Data Accessed: <http://cedar.openmadrigal.org/>, <https://data.amisr.com/database/> ASI Data Accessed: <ftp://optics.gi.alaska.edu/PKR/>

References

- [1] Su, Y., S. Datta-Barua, G. S. Bust, and K. B. Deshpande (2017), Distributed sensing of ionospheric irregularities with a GNSS receiver array, *Radio Sci.*, 52, 988-1003, doi:10.1002/2017RS006331.
- [2] S. Datta-Barua, P. Llado, and D. L. Hampton (2021), Multiyear detection, classification and hypothesis of ionospheric layer causing GNSS scintillation, *Radio Science*.
- [3] Sreenivash, V., Su, Y., & Datta-Barua, S. (2020), Automated ionospheric scattering layer hypothesis generation for detected and classified auroral GPS scintillation events. *Radio Science*, 55, e2018RS006779. <https://doi.org/10.1029/2018RS006779>
- [4] English, A., Stuart, D. J., Hampton, D. L., & Datta-Barua, S. (2024), Automated Nighttime Cloud Detection Using Keograms when Aurora is Present. *Earth and Space Science*, 11. doi:10.1029/2022EA002808
- [5] The Poker Flat Incoherent Scatter Radar (PFISR). AMISR Radar. Retrieved: Mar. 2023. https://amisr.com/amisr/about/about_pfisr/
- [6] Hampton, D. (2024) Optics. <http://optics.gi.alaska.edu/optics/> Scintillation data for saga can be found at: <http://apollo.tbc.iit.edu/~spaceweather/live/?q=SAGA>
- [7] Space Weather Prediction Center. (2024). Aura Tutorial. Retrieved from <https://www.swp.noaa.gov/content/aurora-tutorial> (accessed: 06.04.2023)